Sgr A* Multiwavelength Observations from Radio to X-Ray: Testing Gravity via Accretion onto Black Hole Mimickers

Michael Florian Wondrak
michael@wondrak.info

Anton Pannekoek Institute for Astronomy, University of Amsterdam & GRAPPA, University of Amsterdam

Netherlands Astronomy Conference 2026

Egmond aan Zee, 12 May 2026

in collaboration with H. Olivares, J. Daas, F. Saueressig, and H. Falcke.

J. Daas, K. Kuijpers, F. Saueressig, M.F. Wondrak, H. Falcke, Astron. Astrophys. 673 (2023) A53. arXiv:2204.08480 [gr-qc].
H. Olivares Sanchez, M.F. Wondrak, J. Daas, F. Saueressig, H. Falcke, in preparation.

Outline

- Quadratic gravity (QG)
- Phase space of compact objects
- Optically thin emission model (analytic)
- Magnetized accretion model (fully covariant MHD)
- Outlook

Shadow Observations by the EHT

Shadow of the supermassive black holes M87* and Sgr A* as observed by the Event Horizon Telescope.

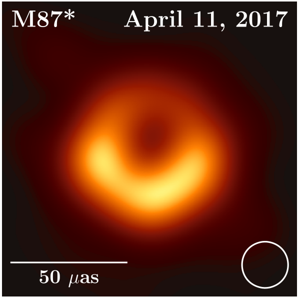

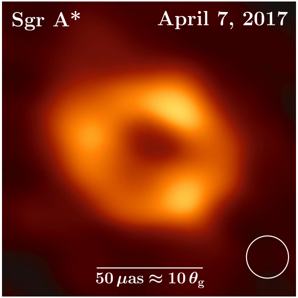

Ring-like shape and central brightness depression: $f_c = T_{b,\ \mathrm{center}} / T_{b,\ \mathrm{ring}}$
Current bounds: $f_c \leq 0.1$ (M87*), $f_c \leq 0.3$ (Sgr A*).

EHTC, Astrophys. J. Lett. **875** (2019) L1; EHTC, Astrophys. J. Lett. **930** (2022) L12

Spectral Energy Distribution (SED) of Sgr A*

Circles indicate multiwavelength observations during EHT campaign.

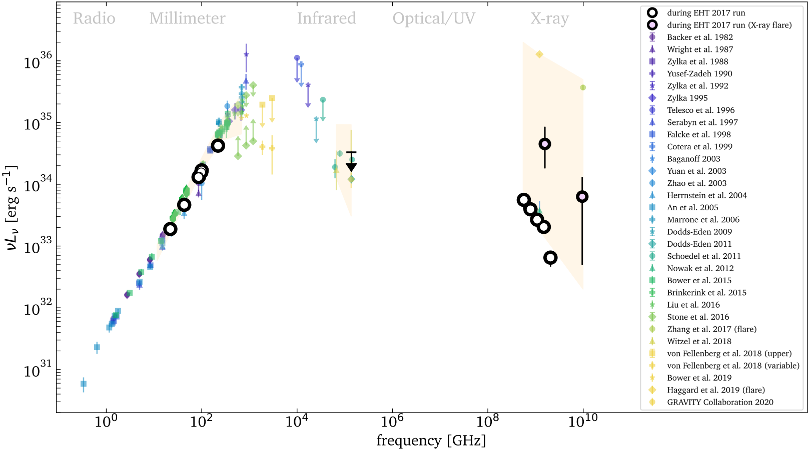

EHTC, Astrophys. J. Lett. **875** (2019) L2

Quadratic Gravity

- General relativity has been tested over the largest range of magnitudes. Still it is conceptually incomplete at the quantum level.
- A theory of quantum gravity is supposed to allow a curvature expansion in the classical limit.
- First-order correction to the GR action arises at quadratic order in curvature (4^{th} order in derivatives). $\rightarrow$ Quadratic gravity.
- Can such corrections be constrained from black-hole shadow and spectral energy distribution observations?

Stelle, Phys. Rev. **D16** (1977) 953; Stelle, Gen. Rel. Grav. **9** (1978) 353

Quadratic Gravity

- Quadratic gravity action in 3+1 dimensions (w/o topological Gauss–Bonnet term):

$$S = \frac{1}{16\pi} \int \mathrm{d}^4x \sqrt{-g} \left[\gamma R - \alpha C_{\mu\nu\rho\sigma} C^{\mu\nu\rho\sigma} + \beta R^2 \right]$$

$C_{\mu\nu\rho\sigma}$: Weyl tensor (change in shape $\rightarrow$ spin-2), R: Ricci scalar (change in volume $\rightarrow$ scalar), α, β: coupling parameters, $\gamma = 1/G$: inverse gravitational constant.

Perturbatively renormalizable QFT, prototype of a quantum theory of gravitational interactions.

- Extension of the Einstein field equations:

$$\gamma \left(R_{\mu\nu} - \frac{1}{2} R\, g_{\mu\nu} \right) - 4\alpha \left(D^\rho D^\sigma + \frac{1}{2} R^{\rho\sigma} \right) C_{\mu\rho\nu\sigma} + 2\beta \left(R_{\mu\nu} - \frac{1}{4} R\, g_{\mu\nu} - D_\mu D_\nu + g_{\mu\nu} D^2 \right) R = 8\pi\, T_{\mu\nu}$$

- We investigate compact objects subject to the vacuum field equations (like black holes in GR).

Stelle, Phys. Rev. **D16** (1977) 953; Stelle, Gen. Rel. Grav. **9** (1978) 353

Compact Objects

- Static, spherically symmetric, asymptotically flat vacuum solutions.
- Metric ansatz:

$$ds^2 = -h(r)\,\mathrm{d}t^2 + \frac{\mathrm{d}r^2}{f(r)} + r^2\left(\mathrm{d}\theta^2 + \sin^2\theta\,\mathrm{d}\phi^2\right)$$

1) Weak field (large r), linearized theory: Yukawa terms.

$$h(r) = 1 - \frac{2M}{r} + 2S_2^- \frac{e^{-m_2 r}}{r} + S_0^- \frac{e^{-m_0 r}}{r}$$

$$f(r) = 1 - \frac{2M}{r} + S_2^- \frac{e^{-m_2 r}}{r}(1 + m_2 r) - S_0^- \frac{e^{-m_0 r}}{r}(1 + m_0 r)$$

$$(m_2)^2 = \frac{\gamma}{2\alpha}, \qquad (m_0)^2 = \frac{\gamma}{6\beta}$$

2) Strong field (small r), Frobenius ansatz: Indicial exponents.
3) Global solution, numerics: Integrate the nonlinear field equations inward.
4) Classify numerical solution according to small r scaling.

Stelle, Gen. Rel. Grav. **9** (1978) 353; Holdom, Phys. Rev. **D66** (2002) 084010

Compact Objects

Birkhoff's theorem from GR does not apply.
$\rightarrow$ Rich phase space of solutions.

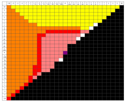

(S_0^-, S_2^-) plane

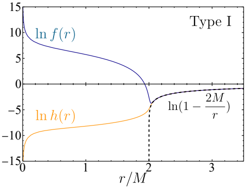

(rose, red, orange)
Type I (naked singularity)
scaling behavior:
$(s, t)_0 = (-2, 2)_0$

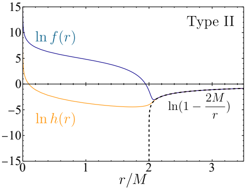

(yellow)
Type II (naked singularity)
scaling behavior:
$(s, t)_0 = (-1, -1)_0$

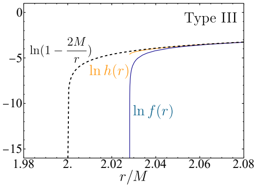

(black)
Type III (wormhole)
scaling behavior:
$(s, t)_{r_0} = (1, 0)_{r_0}$

Stelle, Gen. Rel. Grav. **9** (1978) 353; Holdom, Phys. Rev. **D66** (2002) 084010;
Lü, Perkins, Pope, Stelle, Phys. Rev. **D92** (2015) 124019

Compact Objects

Refining naked singularities of Type I according to the effective potential for massless particles:

$$V_{\text{eff}} = h(r)/r^2$$

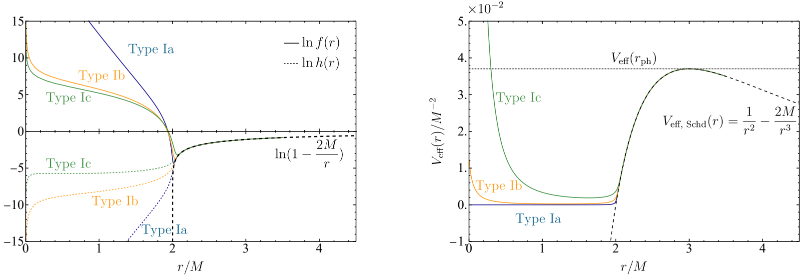

Phase Space of Solutions

Logarithmic (S_0^-, S_2^-) plane

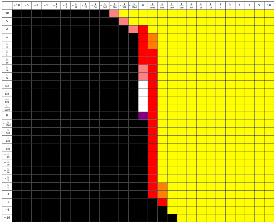

$\alpha = 1/2,\ \beta = 1/3$

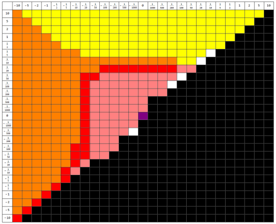

$\alpha = 1/2,\ \beta = 1/6$

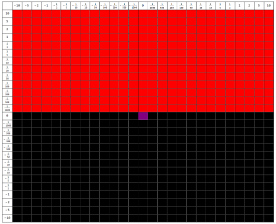

$\alpha = 1/2,\ \beta = 1/18$

Schwarzschild:	Type Ia:	Type Ib:	Type Ic:
Type II:	Type III:	Num. inconclusive:	

$\gamma = 1,\ M = 10,\ r_i = 35$

Type Ia, Ib (naked singularity), III (wormhole)

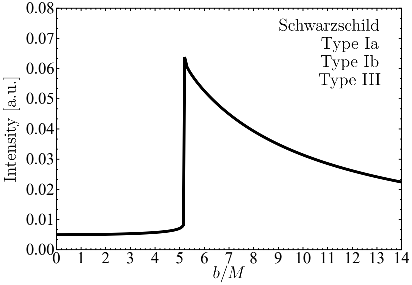

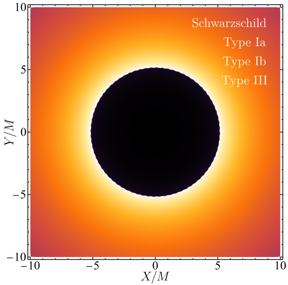

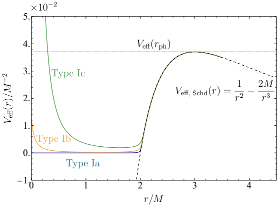

Assumption:
Emission coefficient $j_\nu(\nu_e) \propto \delta(\nu_e - \nu_*)/r^2$

Indistinguishable from Schwarzschild.

Type Ic (naked singularity)

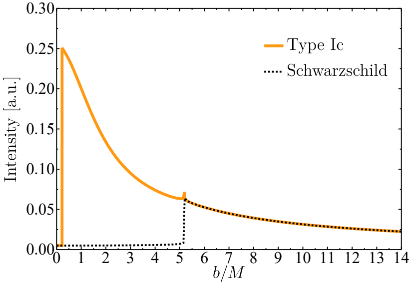

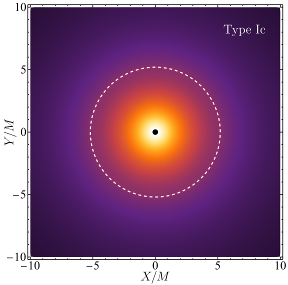

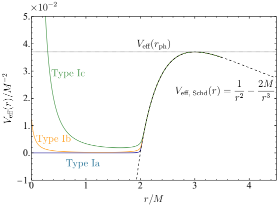

Assumption:
Emission coefficient $j_\nu(\nu_e) \propto \delta(\nu_e - \nu_*)/r^2$

Reduced shadow size.
Peak from the photon sphere provides an intrinsic scale.

Type II (naked singularity)

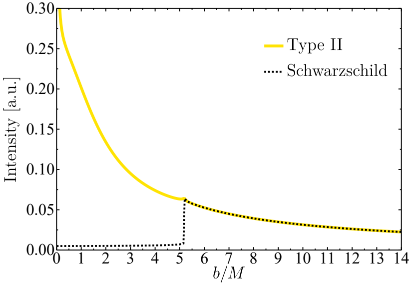

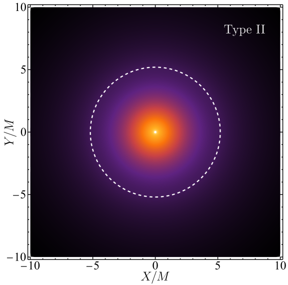

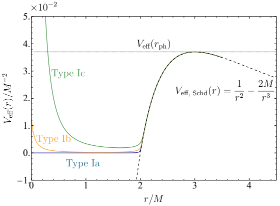

Assumption:
Emission coefficient $j_\nu(\nu_e) \propto \delta(\nu_e - \nu_*)/r^2$

No shadow.
$\rightarrow$ Excluded based on EHT observations.

Local Potential Energy

Model of matter accretion:

Expect dynamics towards decreasing local potential energy.

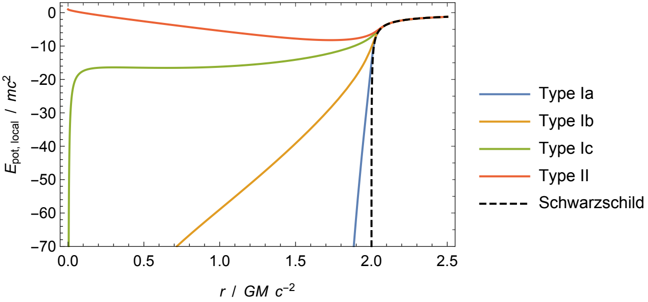

Naked singularities of Type I: attractive, Ia > Ib > Ic.

Naked singularities of Type II: repulsive.

Magnetized Accretion Model

- Initial conditions similar to EHT library:
  SANE torus in hydrodynamic equilibrium, poloidal magnetic field.
  Pressure perturbed by 4% white noise.
- 2-dimensional simulation with BHAC, $N_r \times N_\theta = 96 \times 48$ plus adaptive mesh refinement.
- Passive tracer to keep atmosphere from accumulating in the center.
- Temperature ceiling ($T \lesssim 10^2\, m_\mathrm{p}$) to resemble cooling mechanisms.

Cross Section of Accretion Flow (Type Ib)

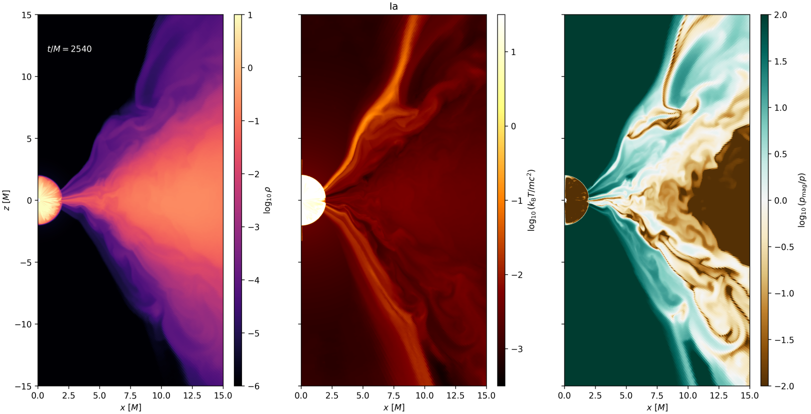

Relative baryon density ρ, dimensionless temperature $T\,/\,m_\mathrm{p}$, inverse plasma-β: $p_\mathrm{mag}\,/\,p_\mathrm{th}$.

Type Ib/Ic/II: Matter stalls inside of would-be horizon and gets isotropic.
Sharp rise in mass density, temperature, and magnetic field towards center.

$\rightarrow$ Optically thick central region.

Infrared Emission by Central Region

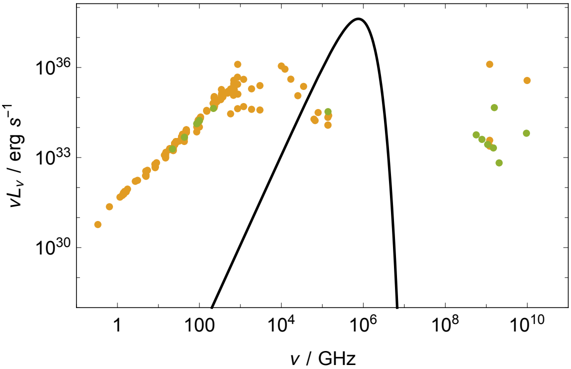

- Black-body emission from central region (hot, optically thick) in addition to synchrotron emission from accretion disk/outflow.

→ Incompatible with observed Sgr A* spectral energy distribution! (orange: pre-2017; green: during 2017 EHT campaign).

Historic data compiled by Zach Sumners.

Conclusions and Outlook

- Survey of Schwarzschild-like solutions in quadratic gravity:

→ Dominated by naked singularities and wormholes.

→ Corrections from quantum gravity at the horizon scale!

- Optically thin emission model:
  A shadow can be present for objects without an event horizon.
- Fully covariant MHD:
  Matter accumulates inside the would-be horizon. Additional thermal radiation component exceeding the SED observations.

→ Constraining the phase space of a quantum-gravity theory by observed shadow size/spectral energy distribution.

- Potentially compatible with observations: Type Ia. (Matter being absorbed faster than potential energy can be released as radiation.)
- Challenging high temperatures reached within would-be horizon.
- 3-dimensional covariant MHD simulations and ray tracing.

Quadratic Gravity

Questions?

michael@wondrak.info